Anisotropy in Thermoelectric Properties of $CsBi_4Te_6$

Duck-Young Chung[1], S. D. Mahanti[2], Wei Chen[3], Citrad Uher[3], Mercouri G. Kanatzidis[1]*
[1]*Department of Chemistry and Center for Fundamental Materials Research, Michigan State University, East Lansing, MI 48824, USA*
[2]*Department of Physics and Astronomy, Michigan State University, East Lansing, MI 48824, USA*
[3]*Department of Physics, University of Michigan, Ann Arbor, MI 48109, USA.*

ABSTRACT

$CsBi_4Te_6$ (ZT ~ 0.8 at 225 K) shows highly anisotropic features in its crystal morphology and structure as expressed by the parallel infinite $[Bi_4Te_6]$ rods which are linked via Bi-Bi bonds. Band calculations also point to a significant anisotropy in the carrier effective masses, and for this reason we examined the anisotropic thermoelectric properties of $CsBi_4Te_6$. The electrical conductivity, thermopower and thermal conductivity were measured along the three different crystallographic directions of the monoclinic structure of $CsBi_4Te_6$. These measurements were performed on samples with different degrees of doping. The strong charge transport anisotropy of these samples was confirmed and also observed that the thermopower values along the c-axis direction (which is perpendicular to the layer of Cs atoms) was negative (-80 μV/K) while those along the needle direction (b-axis) and parallel to the $[Bi_4Te_6]$ layers (a-axis) were p-type (50 – 100 μV/K at room temperature. Other anisotropic features in the crystal growth habit, electronic band structure, and electrical and thermal conductivities are also presented.

INTRODUCTION

Since $CsBi_4Te_6$ suggested as a promising thermoelectric material (ZT ~ 0.8 at 225 K) [1], for low temperature applications, extensive investigations have been performed to understand the material and to improve the thermoelectric properties [2]. The compound crystallizes in a long needle-type morphology reflecting monoclinic unit cell parameters of a = 51.9205(8) Å, b = 4.4025(1) Å, c = 14.5118(3) Å, $\beta = 101.480(1)^o$. The structure features NaCl-type $[Bi_4Te_6]$ slabs that are infinitely extended along the needle axis (b-axis) and Bi-Bi bonds interconnecting the slabs along the a-axis forming layers which are separated by Cs atoms. These morphology and structural characteristics imply highly anisotropic features in its thermoelectric (TE) properties. The TE properties previously reported on $CsBi_4Te_6$ have been performed along the needle (b-) axis since effective charge transport is generally expected to be along this axis.

In order to better understand the properties of this material further investigations of the anisotropy of its physical and thermoelectric properties are necessary. Here, we reports charge transport as well as thermal transport measurements for samples of $CsBi_4Te_6$ along all primary crystallographic directions. The observed results are surprising and are discussed and compared with those predicted from the band structure calculations.

EXPERIMENTAL DETAILS

Three different samples of $CsBi_4Te_6$ were prepared (a) a so-called "as-prepared", (b) Bi-doped, and (c) Sb-doped. The starting materials were appropriately doped (i.e. Bi- and Sb-doped) Bi_2Te_3 which were made by melting a mixture of Bi, Te, and Sb for the nominal composition of Bi_2Te_3, $Bi_{2.05}Te_{2.95}$, and $Bi_2Sb_{0.03}Te_{2.97}$. Cs metal (2.075 g, 15.610 mmol) and a corresponding Bi_2Te_3 (25.0 g, 31.220 mmol) for each doped material were loaded separately in two ends of an H-shaped silica tube. In one leg Bi_2Te_3 was placed. The tube was sealed under vacuum ($<10^{-4}$ Torr) while keeping the Cs containing end in liquid N_2 to avoid evaporation. The tube was heated to 350 ^{o}C over 6 h and isothermed for one day to complete the diffusion of Cs, and then the mixture was heated to 700 ^{o}C over 6 h. After an isotherm at 700 ^{o}C for one day, it was cooled to 450 ^{o}C at a rate of –1 ^{o}C /h. The crystallized material was annealed for one day at 450 ^{o}C and followed by cooling to 50 ^{o}C at a rate of -2 ^{o}C/h. The nominal compositions of the products were $CsBi_4Te_6$, $CsBi_{4.1}Te_6$, and $CsBi_4Sb_{0.06}Te_{5.94.}$ The purity and orientation of the crystals were confirmed by comparison of the X-ray powder diffraction (XRD) pattern and the pattern calculated based on the single crystal structure. The obtained ingot was carefully cut using a wire blade saw for the anisotropic TE property measurements. Approximate dimensions of samples were 7 x 5 x 5 mm^3.

Measurements of conductivity, thermopower and thermal conductivity along all three crystallographic directions were carried out in a cryostat equipped with two radiation shields employing a longitudinal steady-state technique. All measurements were performed in the temperature range of 1.5-300 K. Thermal conductivity data were experimentally corrected for radiation loss. Details of the measurements have been described elsewhere [3].

DISCUSSION

The needle shaped crystals of $CsBi_4Te_6$ tend to grow with the needle axis perpendicular to the temperature gradient of the furnace, see Figure 1. In this study, therefore, the $CsBi_4Te_6$ ingots were grown by a very slow cooling (-1 ^{o}C/h) in a rectangular-shaped silica tube. The cooling rate appeared to be a critical parameter to obtain a high quality crystalline ingot well aligned in one direction. The samples for the charge transport property measurements were obtained from the best grown part of the ingots.

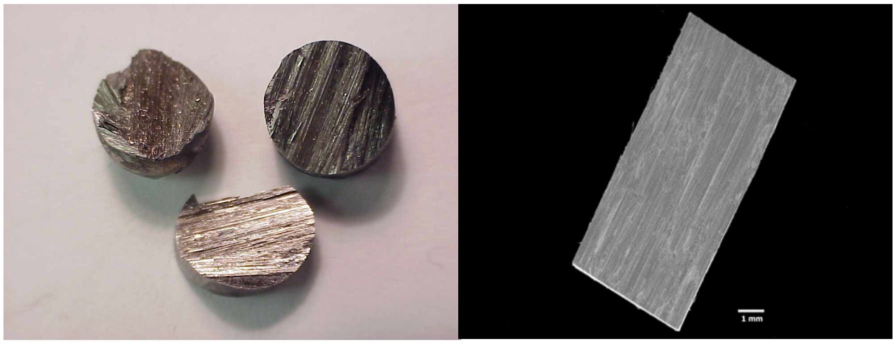

Figure 1. The crystal growth of $CsBi_4Te_6$ perpendicular to the translation axis in a Bridgman furnace is shown in the sliced ingot grown in a cylindrical container (approx 1 cm in diameter) (left) and a sample for TE property measurements was grown by a slow cooling and cut to be a rectangular shape with an approximate dimension of 7 x 5 x 5 mm^3 (right).

$CsBi_4Te_6$ crystallizes in the space group C2/m and presents a unique type of layered structure composed of anionic infinitely long $[Bi_4Te_6]^-$ blocks and Cs^+ ions residing in the interlayer space, see Figure 2. The $[Bi_4Te_6]^-$ block can be regarded as an excised fragment out of the NaCl lattice. This block is two Bi octahedra thick and four Bi octahedra wide (12 x 23 Å^2) in the ac-plane and infinitely long in the b-axis (the needle direction), thus having the shape of an infinite rod that has a rectangular cross section. We emphasize that these slabs are strongly anisotropic to the point that the structure is in essence one-dimensional, and this is consistent with the characteristic needle-like morphology of the crystals. The cleavage of these crystals is strongly preferred along the ab-plane which is the plane accommodating the Cs layers. The $[Bi_4Te_6]^-$ layers consist of only NaCl-type Bi/Te blocks in which inner Bi atoms are coordinated to six Te atoms in a slightly distorted octahedral geometry with distances ranging from 2.974(1) to 3.403(1) Å.

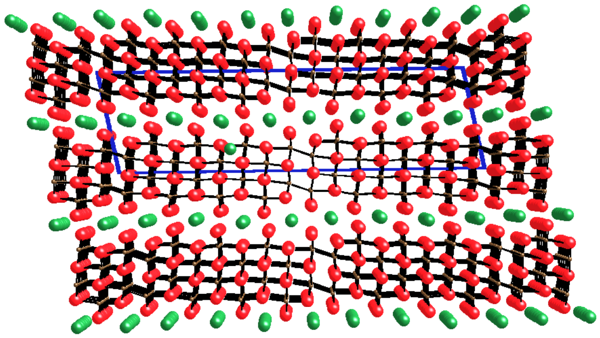

Figure 2. The structure of $CsBi_4Te_6$

The ability of this material to achieve high ZT values at low temperature justifies attempts to understand and rationalize its behavior and properties. The latter are expected to be interesting as suggested by its electronic band structure. Band structure calculations for $CsBi_4Te_6$ were performed without and with a spin-orbit coupling.[4] The spin-orbit coupling shifts the conduction band toward the valence band, resulting in an indirect gap of 0.04 eV placed between the Γ point in the valence band and a general point (C*) in the conduction band, see Figure 3. The band gap of $CsBi_4Te_6$ was observed spectroscopically in the far infrared region to be ~0.1 eV.

The most noteworthy feature in the electronic structure of $CsBi_4Te_6$ is that the compound has a significant anisotropy in carrier effective mass. The anisotropic effective mass influences the B parameter[5] that is a material parameter proportionally related to ZT, as defined as follows :

$$B = \frac{1}{3\pi^2}\left[\frac{2k_BT}{h^2}\right]^{3/2}\frac{\gamma\tau_x}{\kappa_l}\sqrt{\frac{m_y m_z}{m_x}} \qquad \ldots\ldots\ldots\ldots\ldots\ldots (1)$$

where m_x, m_y, and m_z are the effective masses along three principal directions, m_x is the effective mass along the direction of the current flow, γ the band degeneracy, τ_x the scattering time, and κ_l the lattice thermal conductivity. It should be noted in the equation (1) that m_x (the effective mass along the charge transport direction) is inversely related to the parameter B. For an isotropic system where the effective masses along all three directions are similar, B parameter will depend on only one of the effective masses (e.g. m_y) by cancellation of the other two (i.e. m_z/m_x). In contrast, for anisotropic system that the smallest effective masses are on the charge transport direction x and one or both m_y and m_z are large, a large value of the B parameter can be expected. In the band structure of $CsBi_4Te_6$, along the direction (y) parallel to the Bi-Bi bonds the carrier effective mass ($m_y = 1.16$) in valence band is significantly higher than those in all other principal directions ($m_x = 0.02$, $m_z = 0.09$ for valence band, $m_x = 0.04$, $m_y = 0.47$, $m_z = 0.16$ for conduction band). This implies that effective hole transport in the valence band takes place along the direction perpendicular to crystal growth direction (crystallographic b axis) in the plane of Bi/Te slab, eventually leading to a tendency of $CsBi_4Te_6$ to be a p-type material. Also, Bi-Bi bonds are suspected to play a significant role for a high ZT for $CsBi_4Te_6$. Based on these results, the thermoelectric properties along all three directions were examined.

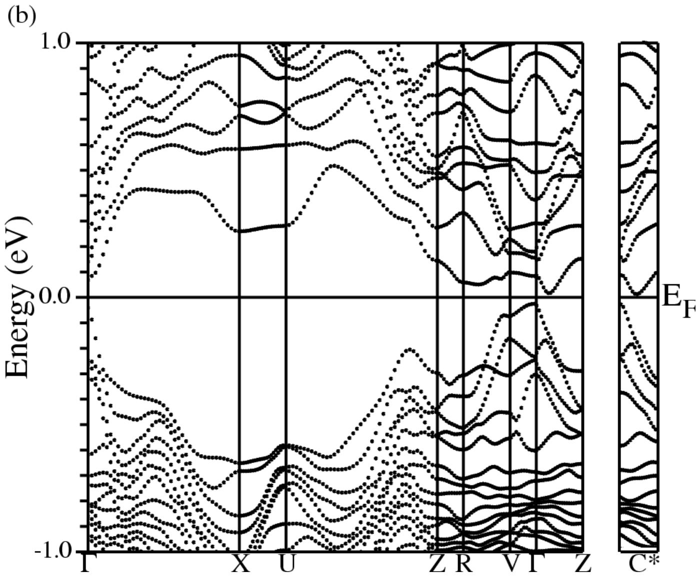

Figure 3. Electronic band structure of $CsBi_4Te_6$ with a spin-orbit coupling.

The thermoelectric properties including conductivity, thermopower, and thermal conductivity of $CsBi_4Te_6$ were measured as described above. The data obtained were verified in terms of the measurement directions by X-ray diffraction patterns taken along each specific direction of the samples. Figure 4 shows the characteristic reflections for each measured direction for the TE properties.

Along the needle direction (b-axis), the room temperature electrical conductivities showed ~2000 S/cm for the as-prepared and Bi-doped samples and ~1000 S/cm for the Sb-doped sample, see Figure 5(A). A relatively large temperature dependence on the conductivities for all three samples combined with the magnitude of thermopower values (+80 −100 V/K) at room temperature suggest the materials are narrow gap conductors with hole carriers in this direction. The thermopower values and thermal conductivity of "as-prepared" $CsBi_4Te_6$ samples are in a good agreement with the reported values in the range of 80 to 120 μV/K and 1.5 – 2.2 W/m-K, respectively, at room temperature. However, based on the magnitudes (~80 μV/K) of thermopower for Bi- and Sb-doped samples which are significantly lower than expected (>130 μV/K at room temperature), these materials appear to have been over-doped during the synthesis.

Perpendicular to the needle direction, which is parallel to the Bi-Bi bonds (a-axis) in the structure, significant changes in all transport properties were observed. By

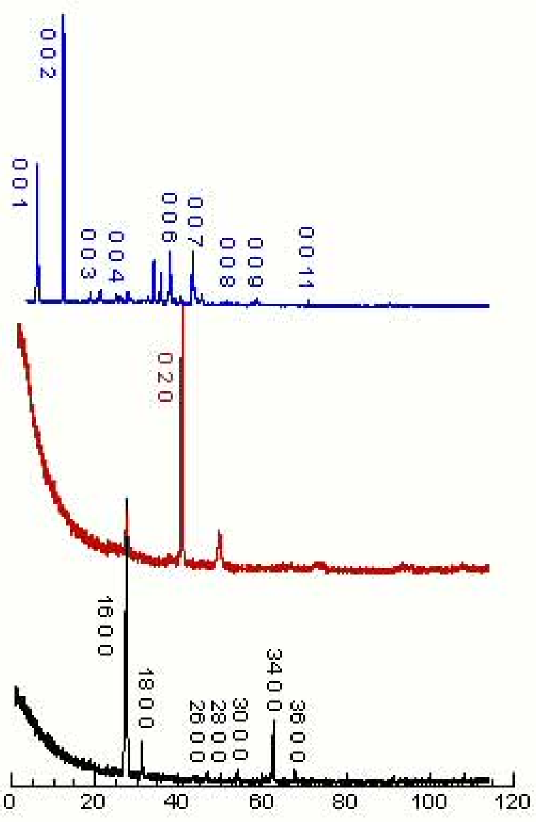

Figure 4. X-ray diffraction pattern of each measured direction of $CsBi_4Te_6$ samples.

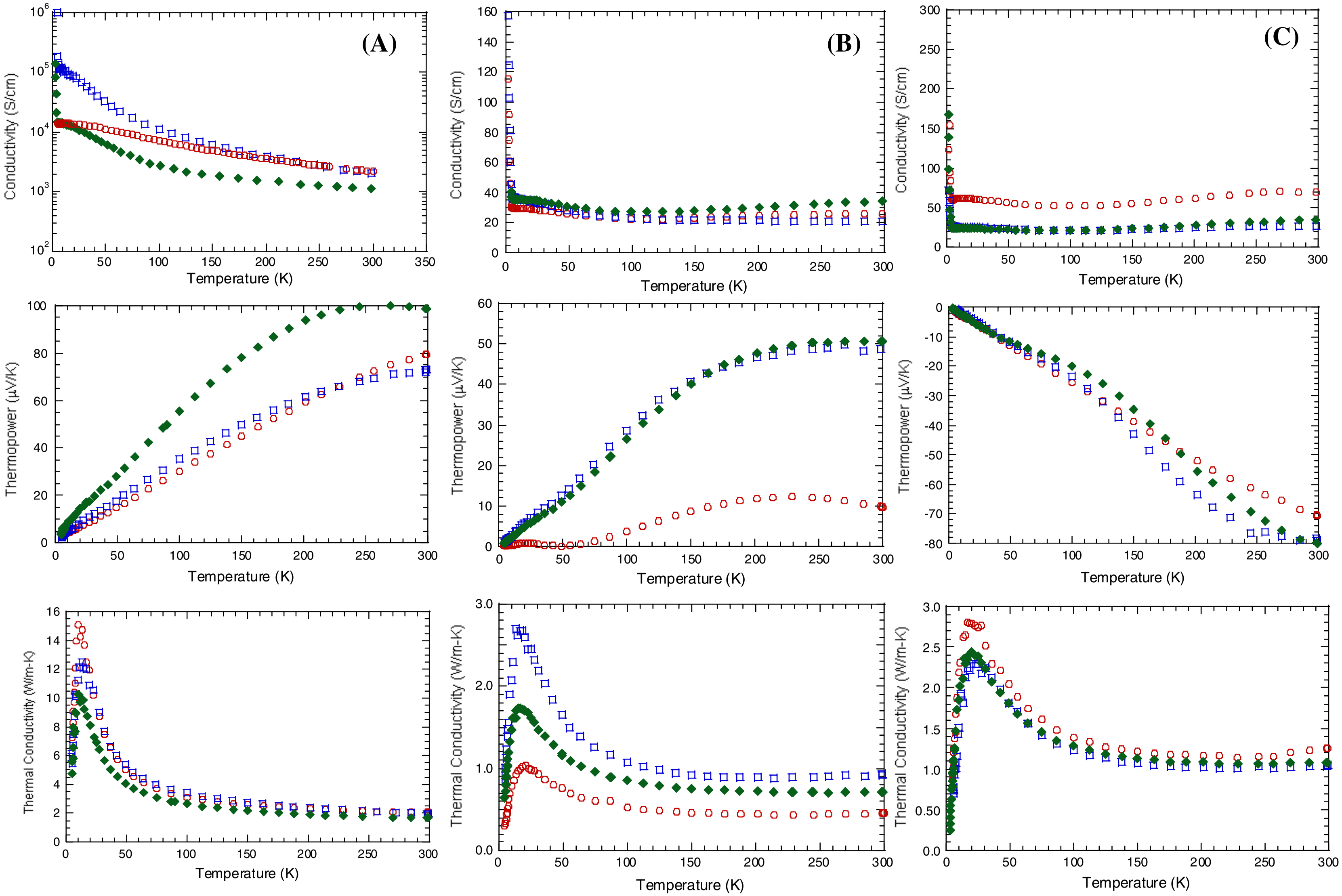

Figure 5. Variable-temperature conductivity, thermopower, and thermal conductivity measured (A) along the needle direction (b-axis) and perpendicular to the needle direction (B) (a-axis) and (C) (c-axis) of $CsBi_4Te_6$ (open circle) as-prepared, (open square) Bi-doped, and (closed diamond) Sb-doped.

comparison to the needle direction (b-axis), the electrical conductivities for all three samples were reduced by two orders of magnitude from ~1000 – 2000 S/cm to ~20 – 40 S/cm at room temperature, see Figure 5(B). Interestingly, the temperature dependence of the electrical conductivity is very weak in the temperature range of 4 – 300 K. Likewise, the thermal conductivity values were found to be half of what was measured along the needle direction. Due to very low electrical conductivities, the electronic contribution to the total thermal conductivity becomes negligible along the a-axis, which is the lowest among all measured directions. The thermopower values are comparable to those in the needle direction (b-axis) with a slight decrease. The as-prepared sample showed the lowest thermopower and thermal conductivity than the other two doped samples. The reason for this phenomenon is not clear yet and will be investigated in near future.

The third direction (along the c-axis) which is perpendicular to the ab-plane and to the [Bi_4Te_6]- slabs in the structure (see Figure 2) showed the most interesting features in this study. The magnitude and behavior of conductivities along the c-axis as a function of temperature are similar to those along a-direction but the thermopower values of all three samples were all negative and similar in magnitude, see Figure 5(C). This negative thermopower is surprising and indicates that the conduction in this direction is carried by a different type of charge carriers (electrons!). A thermopower that changes sign with changing the direction of transport in the same material is a very rare phenomenon. To the best of our knowledge, experimental and theoretical studies for the anisotropic behavior in thermopower for the same compound are limited and have been reported on several high temperature superconducting materials and Bi_2Te_3-related materials [6], of which anisotropy was merely observed by significant changes in magnitude of the thermopower. For $CsBi_4Te_6$, the thermopower values in all three samples consistently show that the major charge carriers in this direction (c-axis) are electrons.

We are currently planning more extensive anisotropic studies on differently doped $CsBi_4Te_6$ including n-doped materials as well as optical spectroscopic studies by a low temperature reflectivity measurements in order to elucidate this very unusual phenomenon.

Given that the negligible electronic thermal conductivity expected (according to Wiedeman-Franz law) due to the very low electrical conductivity (only ~50 S/cm at room temperature) along the c-axis, the total thermal conductivitiy along this direction for all three samples is mostly attributed to the lattice contribution (~1.5 W/m-K at room temperature). Surprisingly, this value is almost as twice as that (~0.85 W/m-K at room temperature) along the needle direction.[1] This suggests that during the crystallization process, $CsBi_4Te_6$ can more effectively dissipate the evolved heat of crystallization to the c-axis than to the needle direction (b-axis), resulting in an abnormal crystal growth habit mentioned above (see Figure 1).

CONCLUSION

Ingots of $CsBi_4Te_6$ “as-prepared”, Bi-doped and Sb-doped show strongly anisotropic TE properties along three principal axes. The magnitudes of TE properties indicate that the materials were heavily doped. In this study, surprisingly the thermopower of all three samples consistently showed a very unusual behavior in which the thermopower is positive along two crystallographic directions but negative along the third which is the direction perpendicular to the $[Bi_4Te_6]$ and Cs^+ layers. We will further investigate this phenomenon through additional experiments. The thermal conductivity of all three samples showed the highest values in the c-direction, explaining the observed unusual crystal growth direction (c-axis) of $CsBi_4Te_6$ as this direction is apparently the direction of most effective heat dissipation.

ACKNLOWEDGMENTS

We gratefully acknowledge the financial support from the Office of Naval Research (Contract No. N00014-01-1-0728).

REFERENCES

1. D.-Y. Chung., T. Hogan, P. Brazis, M. Rocci-Lane, C. R. Kannewurf, M. Bastea, C. Uher, M. G. Kanatzidis, *Science*, **2000**, *287*,1024-1027.
2. (a) P. Larson, S. D. Mahanti, D.-Y. Chung, M. G. Kanatzidis, *Phys. Rev. B*, **2002**, *65*(4), 045205/1-045205/5. (b) P. W. Brazis, M. Rocci, D.-Y. Chung, M. G. Kanatzidis, C. R. Kannewurf, *Mat. Res. Soc. Symp. Proc.*, **1999**, *545*, 75-86. (c) S. Lal, S. Loo, D.-Y. Chung, T. Kyratsi, M. G. Kanatzidis, C. Cauchy, T. P. Hogan, *Mat. Res. Soc. Symp. Proc.*, **2002**, *691*, G6.1.1-6.2.9.
3. J. S. Dyck, W. Chen, C. Uher, Č. Drašar, P. Lošťák *Phys. Rev. B,* **2002***, 66*, 125206.
4. P. Larson, S. D. Mahanti, D-Y Chung, M. G. Kanatzidis, *Phys. Rev. B*, **2001**, *65*, 45205.

5. (a) L. D. Hick, M. S. Dresselhaus, *Phys. Rev. B* **1993**, *47*, 12727. (b) L. D. Hick, M. S. Dresselhaus, *Phys. Rev. B* **1993**, *47*, 16631. (c) L. D. Hick, T. C. Harman, M. S. Dresselhaus, *Appl. Phys. Lett.* **1993**, *63*, 3230.
6. (a) Z. Z. Wang, N. P. Ong, *Phys. Rev. B*, **1988**, *38*, 7160. T. Fujii, I. Terasaki, T. Watanabe, A. Matsuda, *Proc. ISS 2001, Physica C*. (c) X.-F. Chen, G. X. Tessema, M. J. Skove, Phys. Rev. B. **1993**, *48*, 13141. (d) B. Yang, W. L. Liu, J. L. Liu, K. L. Wang, G. Chen, *Appl. Phys. Lett.*, **2002**, *81*, 3588. (e). A. Bilušić, I. Tkalćec, H. Berger, L. Forró. A. Smontara, *FIZIKA A*. (Zagreb), **2000**, *9*, 169.